---

**Article:**
Pang, L.X., Zhou, D., Qi, Z.M. et al. (3 more authors) (2017) Structure–property relationships of low sintering temperature scheelite-structured (1 − x)BiVO 4 –xLaNbO 4 microwave dielectric ceramics. Journal of Materials Chemistry C , 10 (5). pp. 2695-2701. ISSN 2050-7526

https://doi.org/10.1039/C6TC05670A

---

# Structure-property relations of low sintering temperature scheelite-structured $(1-x)BiVO_4$-$xLaNbO_4$ microwave dielectric ceramics

Li-Xia Pang,[a,c] Di Zhou,[*b,c] Ze-Ming Qi,[d] Wei-Guo Liu,[a] Zhen-Xing Yue[e] and Ian M. Reaney[*c]

[a]Micro-optoelectronic Systems Laboratories, Xi'an Technological University, Xi'an 710032, Shaanxi, China

[b]Electronic Materials Research Laboratory, Key Laboratory of the Ministry of Education & International Center for Dielectric Research, Xi'an Jiaotong University, Xi'an 710049, Shaanxi, China

[c]Materials Science and Engineering, University of Sheffield, Sheffield, S1 3JD, UK

[d]National Synchrotron Radiation Laboratory, University of Science and Technology of China, Anhui, 230029, Hefei, China

[e]State Key Laboratory of New Ceramics and Fine Processing, Department of Materials Science and Engineering, Tsinghua University, Beijing 100084, China

[*]Corresponding author. Tel: +86-29-82668679; Fax: +86-29-82668794; E-mail address: zhoudi1220@gmail.com (Di Zhou) & i.m.reaney@sheffield.ac.uk (Ian M. Reaney)

## Abstract

A series of the (1-x)$BiVO_4$-x$LaNbO_4$ ($0.0 \leq x \leq 1.0$) ceramics were prepared via a solid state reaction method. A scheelite-structured solid solution was formed for $x \leq 0.5$ but for $x > 0.5$, tetragonal scheelite, monoclinic $LaNbO_4$-type and $La_{1/3}NbO_3$ phases co-existed. As x increased from 0 to 0.1, the room temperature crystal structure gradually changed from monoclinic to tetragonal scheelite, associated with a decrease in the ferroelastic phase transition temperature from 255 $^oC$ ($BiVO_4$) to room temperature or even below. High sintering temperatures were also found to accelerate this phase transition in compositions with $x \leq 0.08$. Temperature independent high quality factor Qf >10,000 GHz in wide temperature range 25 - 140 $^oC$ and high microwave permittivity $\varepsilon_r \sim 76.3 \pm 0.5$ were obtained for x = 0.06 ceramic sintered at 800 $^oC$. However, small changes in composition resulted in a change in sign and magnitude of the temperature coefficient of resonant frequency (TCF) due to the proximity of the ferroelastic transition to room temperature. If TCF can be controlled and tuned through zero, the (1-x)$BiVO_4$-x$LaNbO_4$ ($0.0 \leq x \leq 1.0$) is a strong candidate for microwave device applications.

# I. Introduction

Bismuth vanadate ($BiVO_4$) has attracted attention due to its novel photocatalytic, dyeing, ferroelastic and dielectric properties, which make it a great candidate in catalyst, pigment and dielectric resonator applications.[1-6] $BiVO_4$ crystallizes in an orthorhombic phase (space group, Pnca [60]) as a natural mineral and takes on a brown color.[7] However, the orthorhombic $BiVO_4$ phase has, to date, never been synthesized. Instead, $BiVO_4$ is readily synthesized in the monoclinic scheelite (I2/b [13]), tetragonal scheelite ($I4_1/a$[88]) and tetragonal zircon-type ($I4_1/amd$ [141]) forms.[1,8,9] Monoclinic scheelite $BiVO_4$ can be prepared via traditional solid state reaction method from $Bi_2O_3$ and $V_2O_5$. However tetragonal scheelite and zircon-structured polymorphs may only be synthesized by soft chemical methods. Critical factors for the successful synthesis of these latter polymorphs includes pH and use of a range and different initial starting materials, such as $Bi(NO_3)_3 \cdot 5H_2O$, $NH_4VO_3$, $HNO_3$, $CH_3COOH$ and NaOH.[5,6] Both the tetragonal scheelite and zircon-type phases are metastable and irreversibly transform to monoclinic scheelite $BiVO_4$ after annealing at high temperature (300 ~ 400 $^oC$).

Monoclinic, tetragonal scheelite $BiVO_4$ and their mixtures are widely used as a Pb-free complex inorganic colored pigment known as C.I. Pigment Yellow 184.[3] Monoclinic scheelite $BiVO_4$ is an n-type photoactive semiconductor with a band gap of 2.4 eV, which has been investigated widely for water splitting applications under visible light.[5,6,10] In addition, monoclinic $BiVO_4$ possesses a high microwave permittivity ($\varepsilon_r$) ~ 68 and quality factor (Qf) ~ 8,000 GHz, which make it a strong candidate for microwave device applications.[11,12]

Monoclinic $BiVO_4$ undergoes a second order reversible ferroelastic phase transition to tetragonal scheelite at 255 $^oC$,[9,13-15] which can be induced by external pressure to

below room temperature.[16] In monoclinic $BiVO_4$, $V^{5+}$ is 4-coordinated and its ionic radius is 0.355 Å. In our previous work,[17-20] single or complex substitutions (~ 10 mol. %) for $V^{5+}$ in $BiVO_4$ using trivalent or hexavalent ions with larger ionic radius, such as $Fe^{3+}$ (0.49 Å), $Mo^{6+}$ (0.41 Å) and $W^{6+}$ (0.41 Å), increased the atomic packing factor of monoclinic scheelite structure, which resulted in an increase in the so-called "internal or chemical pressure", meanwhile lowered the phase transition temperature from 255 $^oC$ to below room temperature. Microwave dielectric properties of scheelite-structured $BiVO_4$ are enhanced by using Li, Mo and Fe, Mo substitutions according to the general formulae $(Li_{0.5x}Bi_{1-0.5x})(Mo_xV_{1-x})O_4$ ($\varepsilon_r$ ~ 81)[17] and $Bi(Fe_{x/3}Mo_{2x/3}V_{1-x})O_4$[20] ($\varepsilon_r$ ~ 75) with Qf > 8,000 and > 13,000GHz, respectively, for compositions near the ferroelastic phase boundary. Highly polarizable B-site ions such as $Ti^{4+}$ and $Nb^{5+}$ have a strong octahedral site preference in many crystal structures.[21,22] In our previous work,[23] $TiO_2$, in which $Ti^{4+}$ resides in octahedral coordination, was found to be immiscible with pure $BiVO_4$, forming a thermodynamically stable composite with $\varepsilon_r$ = 86, Qf = 9,500 GHz and near-zero TCF. Despite the strong octahedral site preference, $Nb^{5+}$ ions in $LaNbO_4$ occupy tetrahedral sites as Kim et al.[24] reporting $\varepsilon_r$ = 19.3, Qf = 54,400 GHz and a TCF ~ + 9 ppm/$^oC$. $LaNbO_4$ has the fergusonite-structure (monoclinic, C2/c) and reversibly transforms to tetragonal scheelite at ~ 480 $^oC$,[25] suggesting that $BiVO_4$-$LaNbO_4$ might, at least in part form a solid solution with useful microwave dielectric properties. Therefore, ceramics in the (1-x)$BiVO_4$-x$LaNbO_4$ ($0.0 \leq x \leq 1.0$) system were prepared via a solid state reaction and their phase evolution, crystal structure, microstructure, and microwave dielectric properties were studied.

## II. Experimental

Proportionate amounts of reagent-grade starting materials of $Bi_2O_3$, $V_2O_5$, $Nb_2O_5$ and $La_2O_3$ (> 99%, Sinopharm Chemical Reagent Co., Ltd, Shanghai, China) were measured according to the stoichiometric formulation $(1-x)BiVO_4$-$xLaNbO_4$ ($0.0 \leq x \leq 1.0$). Details of the processing can be found in our previous work.[18-20] Calcination and sintering temperatures were 680 ~ 800 °C and 780 ~ 1090 °C, respectively. X-ray diffraction (XRD) was performed with Cu Kα radiation (Rigaku D/MAX-2400 X-ray diffractometry, Tokyo, Japan) on crushed powders. Diffraction data werecollected between 2θ of 10 ~ 65° at a step size of 0.02 °. As-fired surfaces was examined by scanning electron microscopy (SEM) (FEI; Quanta 250F). Infrared reflectivity spectra were measured using a Bruker IFS 66v FTIR spectrometer on Infrared beamline station (U4) at the National Synchrotron Radiation Lab. (NSRL), China. Microwave dielectric properties were measured with the $TE_{01\delta}$ dielectric resonator method with a network analyzer (HP 8720 Network Analyzer, Hewlett-Packard) and a temperature chamber (Delta 9023, Delta Design, Poway, CA). The temperature coefficient of resonant frequency TCF ($\tau_f$) was calculated with the following formula:

$$\mathrm{TCF}(\tau_f) = \frac{f_T - f_{T_0}}{f_{T_0} \times (T - T_0)} \times 10^6 \quad (1)$$

where: $f_T$ and $f_{T0}$ were the $TE_{01\delta}$ resonant frequencies at temperature T and $T_0$, respectively.

## III. Results and discussions

Figure 1 presents X-ray diffraction patterns of the $(1-x)BiVO_4$-$xLaNbO_4$ ($0.0 \leq x \leq 1.0$) ceramics calcined and sintered at different temperatures. As shown in Fig. 1 (a), after calcination for 4 h at 680 °C, only peaks associated with a monoclinic scheelite

phase were present for $0.02 \leq x \leq 0.08$. Compared with calcined samples, the (200) and (020) of x = 0.04 and 0.06 ceramics sintered 2 h at 780 $^{o}$C begin to converge, suggesting that the distortion of $BO_4$ tetrahedra decreases at high sintering temperature. Besides, as shown in Fig. S1 (Supporting Information), atomic packing factor increased slightly with x value and reached a maximum value about 62.9 % at x =0.08 and 0.10. The (200/020) peaks were still separate for x = 0.08 (680 $^{o}$C) but at higher temperature (710 $^{o}$C) they almost merged into a single peak, as shown in Fig. 1 (c), implying that the structure transformed from a monoclinic to tetragonal scheelite, thus illustrating the sintering temperature and compositional dependence of the ferroelastic transition temperature. The changes in the structure as a function of sintering temperature most likely relate to the rate diffusion and / or solid solubility of Nb in V tetrahedral network. $Nb_2O_5$ is a comparatively refractory oxide and a homogeneous distribution is difficult to obtain at low sintering temperatures. As sintering temperature increases, Nb distributes more uniformly, resulting in convergence of the (200)/(020) peaks. Moreover, the solid solubility of La and Nb ions may increase with sintering temperature. We note that the effect of sintering temperature on the ferroelastic transition temperature is negligible in other $BiVO_4$ based solid solutions, such as the $(Li_{0.5x}Bi_{1-0.5x})(Mo_xV_{1-x})O_4$, $(Na_{0.5x}Bi_{1-0.5x})(Mo_xV_{1-x})O_4$, $(K_{0.5x}Bi_{1-0.5x})(Mo_xV_{1-x})O_4$ and $(Ag_{0.5x}Bi_{1-0.5x})(Mo_xV_{1-x})O_4$ systems,[17-19] presumably because of the less refractory nature of these solid solutions. A schematic of the $ABO_4$ scheelite structure and an illustration of how Nb reduces the distortion of the tetrahedra and related cell parameters are plotted in Fig.1 (e) and (f). The presence of $La_{1/3}NbO_3$ in XRD traces for samples with $x < 0.70$ indicates that there is limited solid solubility of La and Nb ions in the scheelite structured solid solution in the $(1-x)BiVO_4$-$xLaNbO_4$ ($0.0 \leq x \leq 1.0$) ceramics. For x = 0.90,

monoclinic $LaNbO_4$ was observed as the main phase but nonetheless peaks associated with $La_{1/3}NbO_3$ were present in XRD traces.[26] The ionic radius of 8-coordinated $La^{3+}$ and 4-coordinated $Nb^{5+}$ are 1.16 Å (a little smaller than that of $Bi^{3+}$, 1.17 Å) and 0.48 Å, respectively (much larger than that of $V^{5+}$, 0.355 Å).[27] As shown in Fig. 1 (f), both the a/b ratio and cell volume of tetragonal scheelite phase increase linearly with increase of content of $LaNbO_4$, which corresponds well with our previous results in other $BiVO_4$-based solid solutions.[20,21] Pure $LaNbO_4$ is fergusonite-structured (monoclinic, C2/c)[25] and undergoes a ferroelastic phase transition to tetragonal scheelite structure at high temperature. The large difference in cell parameters is most likely responsible for the limited solid solubility of $LaNbO_4$ in $BiVO_4$.

The symmetry of monoclinic scheelite-structured $BiVO_4$ is I2/b and it gives nine Raman active modes according to group theory:[28,29]

$$\Gamma = 3A_g + 6B_g \quad (2)$$

Room temperature Raman spectra of the (1-x)$BiVO_4$-x$LaNbO_4$ (x = 0.02, 0.04, 0.06, 0.08 and 0.10) ceramics are shown in Fig. 2. The strongest mode at about 825 $cm^{-1}$ is assigned to the symmetric V–O stretching mode ($v_s$(V–O)) and the weaker one at about 725 $cm^{-1}$ to an asymmetric V–O stretching mode ($v_{as}$(V–O)). Raman modes at about 331 and 366 $cm^{-1}$ are assigned to asymmetric and symmetric bending modes $\delta_{as}(VO_4)$ and $\delta_s(VO_4)$, respectively. The modes below 250 $cm^{-1}$ are external rotation / translation modes, strongly related to A site ions. Key evidence supporting the phase evolution from monoclinic to the tetragonal scheelite structure is the gradual merging of $\delta_{as}(VO_4)$ and $\delta_s(VO_4)$ with increase of x as marked in Fig. 2 (a) and plotted in Fig. 2 (b), caused by a reduction in distortion of the $BO_4$tetrahedra. As shown in Fig. 2 (b), the stretching mode $v_s$(V–O) red-shifted with the increase of x value in the (1-x)$BiVO_4$-x$LaNbO_4$. The stretching mode is strongly related with the B-O bond

length. Hardcastle and Wachs gave a empirical relation between Raman shift and V-O bond length in 1991:[30]

$$\nu = 21349 \times \exp(-1.9176R), \quad (3)$$

where ν is the Raman shift in $cm^{-1}$ and R is the V−O bond length in Å. The calculated B-O bond length is also plotted in Fig. 2 (b). It is only an approximate calculation due to the existence of $NbO_4$ tetrahedra but the substitution of Nb for V increases the B-O bond length, in agreement with the XRD results.

Un-doped $BiVO_4$ and $LaNbO_4$ densify at 800 ºC and 1250 ºC, respectively.[11,24] Optimum sintering temperature of the (1-x)$BiVO_4$-x$LaNbO_4$ ceramics remained around 800 ºC when $x \leq 0.10$ but then increased to 1090 ºC at x= 0.90. SEM images of the (1-x)$BiVO_4$-x$LaNbO_4$ ceramics with $0.02 \leq x \leq 0.10$ sintered at their optimal temperature are shown in Fig. 3. Dense and homogeneous microstructures were observed for all the samples. Substitution of $LaNbO_4$ into $BiVO_4$ restricted grain growth from > 5 μm for x = 0.02 composition to below 5 μm for x = 0.06 sintered at 800 ºC. With further increase of $LaNbO_4$ concentration, optimal sintering temperature increased and the grain size increased to > 5 μm for x = 0.10 ceramic sintered at 820 ºC.

$\varepsilon_r$ and Qf of the (1-x)$BiVO_4$-x$LaNbO_4$ ceramics as a function of x are shown in Fig. 4 (a). $\varepsilon_r$ increased linearly from 68 at x = 0 to 80 at x = 0.10 within the monoclinic scheelite solid solution region and then decreased to ~ 30 for x = 0.90. Qf followed a similar trend as a function of x with values > 8,000 GHz for $0 \leq x \leq 0.1$ in the monoclinic scheelite phase region but for x > 0.1, Qf decreased sharply to below 3,000 GHz for x = 0.9 sample. Although $LaNbO_4$ is reported to possess a high Qf value ~ 54,400 GHz,[24] the poor Qf value for x = 0.9 might be attributed to the existence of the $La_{1/3}NbO_3$ phase.[31,32] The large permittivity and Qf values of

monoclinic structured compositions are attributed to their high atomic packing factor[17-20] which is a maximum for x = 0.1 in the (1-x)$BiVO_4$-x$LaNbO_4$ system as shown in Fig. S1 from "Supporting Information". Consequently, there is a decrease in Qf and $\varepsilon_r$ for higher values of x, although the existence of secondary phases may also increase microwave dielectric loss.

$\varepsilon_r$ as a function of temperature from 25 ~ 140 $^oC$ for x = 0.04, 0.06, and 0.10 is shown in Fig. 4 (b). For pure $BiVO_4$, the temperature stability is influenced by the ferroelastic transition at ~ 255 $^oC$ which results in a large negative TCF of ~ – 260 ppm/$^oC$ at room temperature. Substitution of $LaNbO_4$ into $BiVO_4$ lowers the phase transition temperature to below room temperature and switches the sign of TCF to + 204 ppm/$^oC$ for x = 0.10, as shown in Fig. 4 (b). $\varepsilon_r$ attains a maximum peak value at 134 $^oC$ for x = 0.04 but for x = 0.06, the phase transition temperature is lowered to ~ 80 $^oC$, which resulted in equivalent TCF $\leq \pm$ 85 ppm/$^oC$. For x = 0.10 sample, no peak in $\varepsilon_r$ was observed between 25 to 140 $^oC$, which indicates that the phase transition temperature was about or below 25 $^oC$, in agreement with XRD data.

For x = 0.10, Qf decreased linearly with temperature to a minimum of 8,000 GHz. For x = 0.04 and x= 0.06 samples, Qf is > 10,000 GHz and stable over a wide temperature range in contrast to ($A_{0.5}Bi_{0.5}$)$MoO_4$ (A = Li, Na, K and Ag) $BiVO_4$ systems,[17-20] in which Qf decreased sharply with increasing temperature. It is concluded that substitution of $La^{3+}$ on A site and $Nb^{5+}$ on B site in scheelite-structured $BiVO_4$ improves the temperature dependence of Qf values and increases $\varepsilon_r$.

Measured and calculated infrared reflectivity spectra (IR) of the (1-x)$BiVO_4$-x$LaNbO_4$ (x = 0.02, 0.04, 0.06, 0.08 and 0.10) ceramics are shown in Fig. 5 (a). Complex reflectivity $R(\omega)$ can be written as:

$$R(\omega) = \left| \frac{1 - \sqrt{\varepsilon^*(\omega)}}{1 + \sqrt{\varepsilon^*(\omega)}} \right|^2 \quad (4)$$

Then IR reflectivity spectra can be analyzed using a classical harmonic oscillator model as follows:

$$\varepsilon^*(\omega) = \varepsilon_\infty + \sum_{j=1}^{n} \frac{\omega_{pj}^2}{\omega_{oj}^2 - \omega^2 - j\gamma_j \omega} \quad (5)$$

where $\varepsilon^*(\omega)$ is the complex dielectric function; $\varepsilon_\infty$ is the dielectric constant caused by the electronic polarization at high frequencies; $\gamma_j$, $\omega_{oj}$, and $\omega_{pj}$ are the damping factor, the transverse frequency, and plasma frequency of the j-th Lorentz oscillator, respectively; and n is the number of transverse phonon modes. As shown in Fig. 5 (a), all spectra fitted well by employing equations (4) and (5). As x increased, along with driving the monoclinic to tetragonal scheelite transition, some vibrational modes below 500 $cm^{-1}$ merged continuously, e.g. $\delta_{as}(BO_4)$ and $\delta_s(BO_4)$ modes. The fitted complex dielectric spectra are shown in Fig. 5 (b) and the experimental values measured in the microwave region are also plotted. Both the fitted and measured values correspond well, which confirms that dielectric polarization at microwave frequencies is dominated by absorption of phonons at the far-infrared region and that there is no contribution from dipolar or other polarization mechanisms. The phonon parameters in the Supporting Information illustrate that external vibrational modes caused by A site ions ($Bi^{3+}$ and $La^{3+}$) contributed mainly (above 85 %) to the dielectric polarization at microwave frequencies. This result also follow Shannon's additive rule in which the polarizability of $Bi^{3+}$ (6.12 $Å^3$) and $La^{3+}$ (6.07 $Å^3$) are much larger than that of $Nb^{5+}$ (3.97$Å^3$) and $V^{5+}$ (2.92 $Å^3$). Although it is difficult to calculate every contribution to the polarization from each vibrational mode at microwave frequencies, both the infrared spectra fitting and Shannon's additive rule give a reasonable

qualitative assessment. Although the vibrational modes caused by tetrahedron bending are characteristic modes to identify the phase transition from monoclinic to tetragonal scheelite structure, their contributions to microwave dielectric permittivity are negligible. Hence, no matter monoclinic or tetragonal models were employed for x = 0.10 composition, there was no remarkable difference observed as shown in Fig. S2, Table S4 and Table S5.

## IV. Conclusions

Scheelite structured solid solution formed in the (1-x)$BiVO_4$-x$LaNbO_4$ ceramics within $0 \leq x < 0.7$. Increasing x and sintering temperature accelerated the monoclinic to tetragonal scheelite phase transition for $x \leq 0.1$. For $x \leq 0.1$, samples could be densified at ~ 800 $^oC$ with a grain size 1 to 5μm. As indicated by Raman spectroscopy, substitution of $Nb^{5+}$ for $V^{5+}$ increased the B-O bond length and drove the monoclinic−tetragonal phase transition to below room temperature. $\varepsilon_r > 75$ with a fluctuation of ~ 1.24 % (TCF ≤ ± 85 ppm/$^oC$) accompanied by a Qf ~ 10,000 GHz in the range 25 ~ 140 $^oC$ were obtained in x = 0.06 ceramic sintered at 800 $^oC$ for 2 h. This novel system extends the understanding of ferroelastic phase transition in scheelite structure materials and provides a promising candidate for low temperature co-fired ceramic technology.

# Acknowledgements

This work was supported by the National Natural Science Foundation of China (U1632146), the Young Star Project of Science and Technology of Shaanxi Province (2016KJXX-34), the Fundamental Research Funds for the Central University, and the 111 Project of China (B14040). The authors would like to thank the administrators in IR beamline workstation of National Synchrotron Radiation Laboratory (NSRL) for their help. The SEM work was done at International Center for Dielectric Research (ICDR), Xi'an Jiaotong University, Xi'an, China and the authors thank Ms. Yan-Zhu Dai for her help in using SEM. Ian M. Reaney would like to acknowledge Engineering and Physical Sciences Research Council grant, EP/N010493/1.

## Refferences


1 A. W. Sleight and W. J. Linn, Ann. N. Y. Acad. Sci., 1976, **272**, 22.

2 M. Valant and D. Suvorov, J. Am. Ceram. Soc., 2000, **83**, 2721.

3 H. Wienand, W. Ostertag and K. Bittler, US Pat. 4455174, 1984.

4 J. A. Seabold and K. S. Choi, J. Am. Chem. Soc., 2012, **134**, 2186.

5 A. Iwase and A. Kudo, J. Mater. Chem., 2010, **20**, 7536.

6 J. Q. Yu and A. Kudo, Adv. Funct. Mater., 2006, **16**, 2163.

7 M. M. Qurashi and W. H. Barnes, Am. Mineral., 1953, **38**, 489−500.

8 J. W. E. Mariathasan, R. M. Hazen and L. W. Finger, Phase Transit., 1986, **6**, 165.

9 A. W. Sleight, H. Y. Chen, A. Ferretti and D. E. Cox, Mater. Res. Bull., 1979, **14**, 1571.

10 G. Kaur, O. P. Pandey and K. Singh, Phys. Status Solidi A, 2012, **209**, 1231.

11 M. Valant and D. Suvorov, J. Am. Ceram.Soc., 2000, **83**, 2721.

12 S. H. Wee, D. W. Kim and S. I. Yoo, J. Am. Ceram. Soc., 2004, **87**, 871.

13 J. D. Bierlein and A. W. Sleight, Solid State Commun., 1975, **16**, 69.

14 W. I. F. David, A. M. Glazer and A. W. Hewat, Phase Transi., 1979, **1**, 155.

15 W. I. F. David and I. G. Wood, J. Phys. C Solid State Phys., 1983, **16**, 5127.

16 R. M. Hazen and J. W. E. Mariathasan, Science, 1982, **216**, 991.

17 D. Zhou, W. G. Qu, C. A. Randall, L. X. Pang, H. Wang, X. G. Wu, J. Guo, G. Q. Zhang, L. Shui, Q. P. Wang, H. C. Liu and X. Yao, Acta Mater., 2011, **59**, 1502.

18 D. Zhou, L. X. Pang, H. Wang, J. Guo, X. Yao and C. A. Randall, J. Mater. Chem., 2011, **21**, 18412..

19 D. Zhou, L. X. Pang, J. Guo, H. Wang, X. Yao and C. A. Randall, Inor. Chem., 2011, **50**, 12733.

20 D. Zhou, L. X. Pang, J. Guo, Z. M. Qi, T. Shao, X. Yao and C. A. Randall, J. Mater. Chem., 2012, **22**, 21412..

21 W. Jauch and A. Palmer, Phys. Rev. B., 1999, **60**, 2961.

22 J. Wu, D. Xiao and J. Zhu, Chem. Rev., 2015, **115**, 2559.

23 D. Zhou, D. Guo, W. B. Li, L. X. Pang, X. Yao, D. W. Wang and I. M. Reaney, J. Mater. Chem. C, 2016, **4**, 5357.

24 D. W. Kim, D. K. Kwon, S. H. Yoon and K. S. Hong, J. Am. Ceram. Soc., 2006, **89**, 3861.

25 K. A. Gingerich and H. E. Bair, Adv. X-Ray Anal., 1964, 7, 22.

26 B. J. Kennedy, C. J. Howard, Y. Kubota and K. Kato, J. Solid State Chem., 2004, **177**, 4552.

27 R. D. Shannon, Acta Crystallogr. Sect. A., 1976, **A32**, 751.

28 R. L. Frost, D. A. Henry, M. L. Weier and W. Martens, J. Raman Spectrosc., 2006, **37**, 722.

29 M. S. Jang, H. L. Park, J. N. Kim, J. H. Ro and Y. H. Park, Jpn. J. Appl. Phys., 1985, **24**, 506.

30 F. D. Hardcastle and I. E. Wachs, J. Phys. Chem., 1991, **95**, 5031.

31 T. Mondal, P. M. Sarun, S. Das and T. P. Sinha, AIP Conference Proceedings, 2015, **1665**, 110043.

32 A. Mikonis, J. Macutkevic, R. Grigalaitis, J. Banys, R. Adomavicius, A. Krotkus, A. N. Salak, N. P. Vyshatko and D. D. Khalyavin, Integrated Ferroelec., 2009, **109**, 55.

# Figure Captions:

**Fig. 1** X-ray diffraction patterns of the (1-x)$BiVO_4$-x$LaNbO_4$ ($0.0 \leq x \leq 1.0$) ceramics calcined (a) and sintered (b), (c), (d) at different temperatures, schematic of $ABO_4$ scheelite structure (release of distorted tetrahedral in insert) (e), and cell parameters of the main phases as a function of x value (* — monoclinic scheelite phase, o — tetragonal scheelite phase, L — monoclinic $LaNbO_4$ phase, v — $La_{1/3}NbO_3$ phase)

**Fig. 2** Room-temperature Raman spectra of the (1-x)$BiVO_4$-x$LaNbO_4$ (x=0.02, 0.04, 0.06, 0.08 and 0.10) ceramics sintered at their optimal temperatures

**Fig. 3** SEM images of the (1-x)$BiVO_4$-x$LaNbO_4$ ceramics (a) for x=0.02 sintered 2 h at 780 $^oC$, (b) for x=0.04 sintered 2 h at 800 $^oC$, (c) for x=0.06 sintered 2 h at 800 $^oC$, and (d) for x=0.10 sintered 2 h at 820 $^oC$

**Fig. 4** Microwave dielectric permittivity and Qf values of the (1-x)$BiVO_4$-x$LaNbO_4$ ceramics as a function of x value (a) and temperature (b) in range 25 ~ 140 $^oC$

**Fig. 5** Measured and calculated infrared reflectivity spectra of the (1-x)$BiVO_4$-x$LaNbO_4$ (x=0.02, 0.04, 0.06, 0.08 and 0.10)ceramics (a) (solid line for fitting values and circle for measured values) and their complex dielectric spectra (b) (circles are experimental at microwave region, solid lines represent the fit of IR spectra)

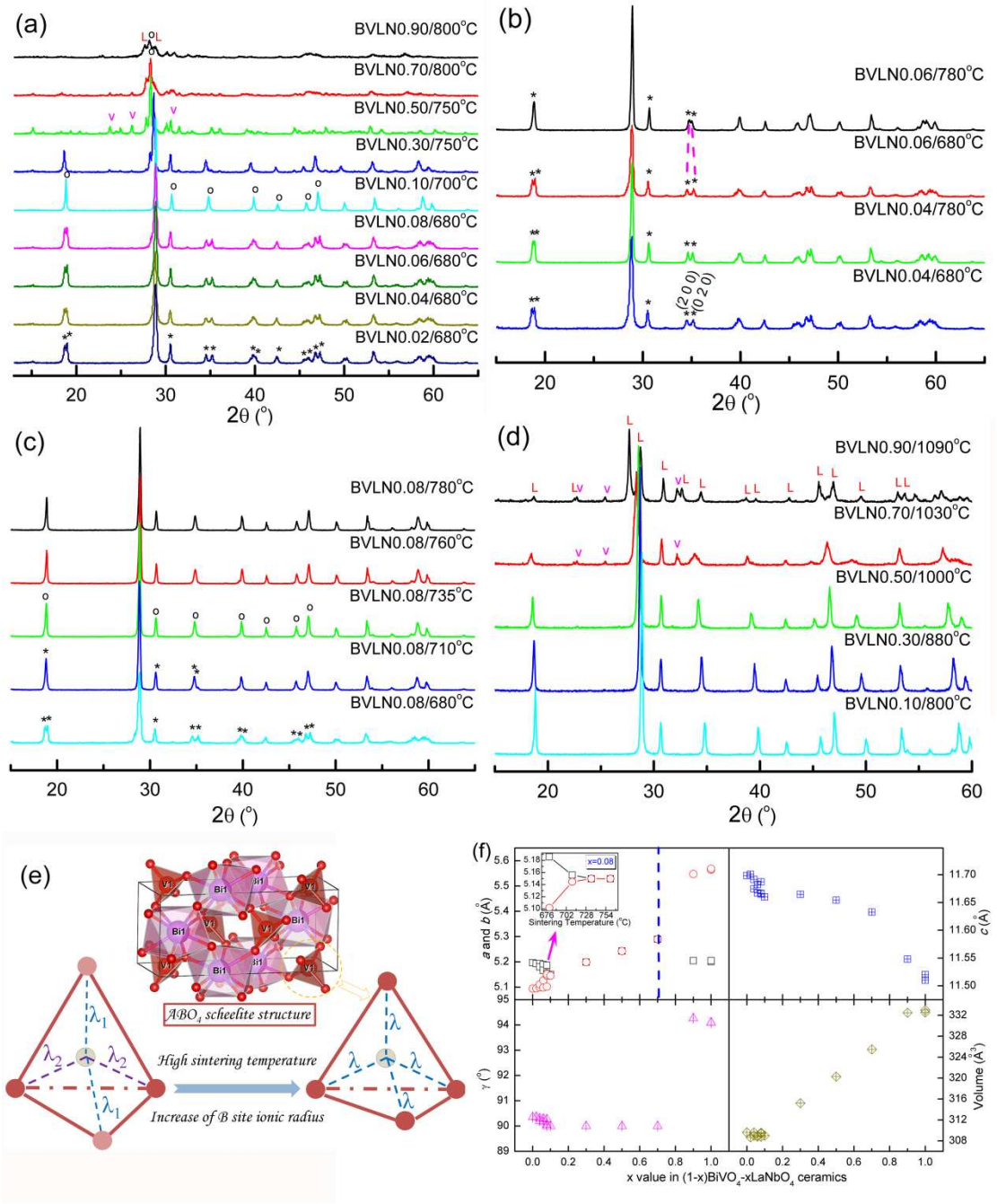


**Fig. 1** X-ray diffraction patterns of the (1-x)$BiVO_4$-x$LaNbO_4$ ($0.0 \leq x \leq 1.0$) ceramics calcined (a) and sintered (b), (c), (d) at different temperatures, schematic of $ABO_4$ scheelite structure (release of distorted tetrahedral in insert) (e), and cell parameters of the main phases as a function of x value (f) (* — monoclinic scheelite phase, o — tetragonal scheelite phase, L — monoclinic $LaNbO_4$ phase, v — $La_{1/3}NbO_3$ phase)

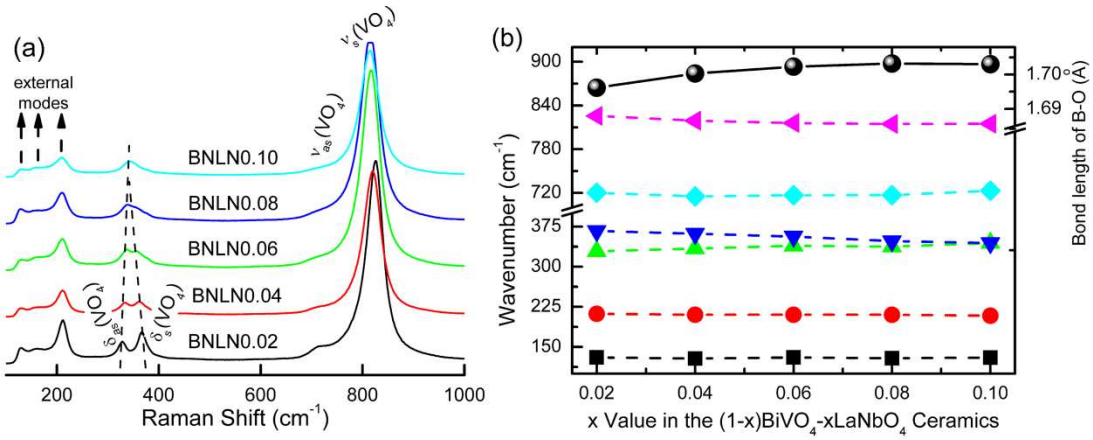


**Fig. 2** Room-temperature Raman spectra of the (1-x)$BiVO_4$-x$LaNbO_4$ (x=0.02, 0.04, 0.06, 0.08 and 0.10) ceramics sintered at their optimal temperatures

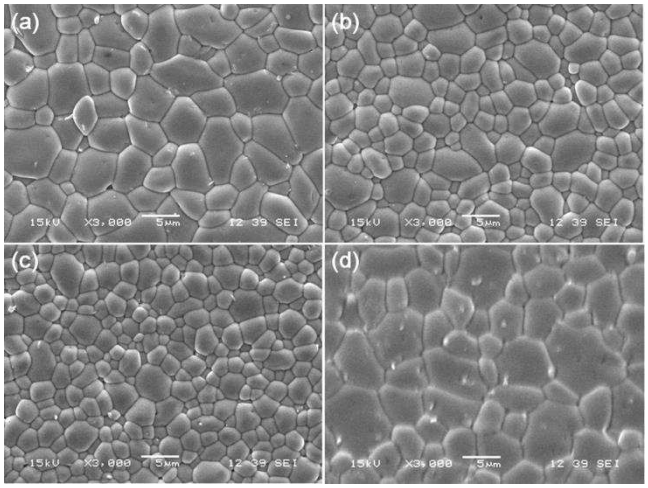


**Fig. 3** SEM images of the (1-x)$BiVO_4$-x$LaNbO_4$ ceramics (a) for x=0.02 sintered 2 h at 780 $^oC$, (b) for x=0.04 sintered 2 h at 800 $^oC$, (c) for x=0.06 sintered 2 h at 800 $^oC$, and (d) for x=0.10 sintered 2 h at 820 $^oC$

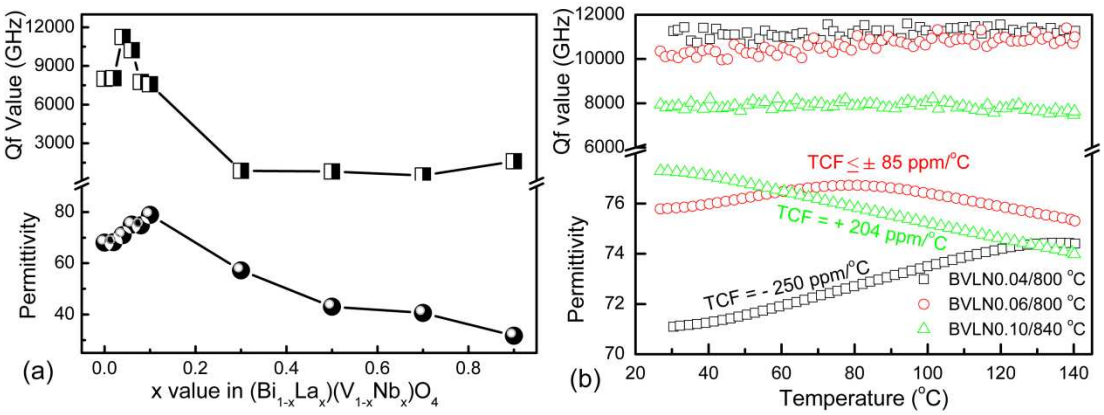


**Fig. 4** Microwave dielectric permittivity and Qf values of the (1-x)$BiVO_4$-x$LaNbO_4$ ceramics as a function of x value (a) and temperature (b) in range 25 ~ 140 ºC

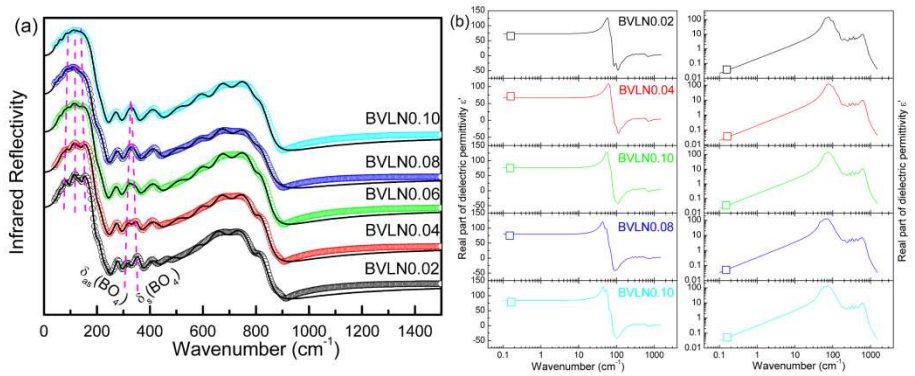


**Fig. 5** Measured and calculated infrared reflectivity spectra of the (1-x)$BiVO_4$-x$LaNbO_4$ (x=0.02, 0.04, 0.06, 0.08 and 0.10)ceramics (a) (solid line for fitting values and circle for measured values) and their complex dielectric spectra (circles are experimental at microwave region, solid lines represent the fit of IR spectra)

# Table of Contents

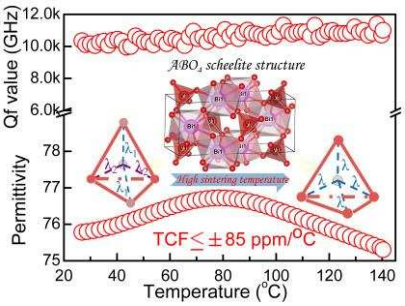


Permittivity ~ 76.3 ± 0.5 and quality factor > 10,000 GHz were obtained in $0.94BiVO_4$-$0.06LaNbO_4$ ceramic sintered at 800 °C.